

# I Gede Artha Negara

## IJAME\_Rev.docx

 Politeknik Negeri Bali

---

### Document Details

Submission ID

trn:oid:::3618:81504874

Submission Date

Feb 9, 2025, 12:38 PM GMT+8

Download Date

Feb 9, 2025, 12:44 PM GMT+8

File Name

IJAME\_Rev.docx

File Size

9.1 MB

20 Pages

7,893 Words

45,776 Characters

# 19% Overall Similarity

The combined total of all matches, including overlapping sources, for each database.

## Filtered from the Report

- Bibliography

## Match Groups

-  **101** Not Cited or Quoted 18%  
Matches with neither in-text citation nor quotation marks
-  **12** Missing Quotations 2%  
Matches that are still very similar to source material
-  **0** Missing Citation 0%  
Matches that have quotation marks, but no in-text citation
-  **0** Cited and Quoted 0%  
Matches with in-text citation present, but no quotation marks

## Top Sources

- 9%  Internet sources
- 11%  Publications
- 14%  Submitted works (Student Papers)

## Integrity Flags

### 1 Integrity Flag for Review

-  **Hidden Text**  
15 suspect characters on 1 page  
Text is altered to blend into the white background of the document.

Our system's algorithms look deeply at a document for any inconsistencies that would set it apart from a normal submission. If we notice something strange, we flag it for you to review.

A Flag is not necessarily an indicator of a problem. However, we'd recommend you focus your attention there for further review.

### Match Groups

- **101** Not Cited or Quoted 18%  
Matches with neither in-text citation nor quotation marks
- **12** Missing Quotations 2%  
Matches that are still very similar to source material
- **0** Missing Citation 0%  
Matches that have quotation marks, but no in-text citation
- **0** Cited and Quoted 0%  
Matches with in-text citation present, but no quotation marks

### Top Sources

- 9% Internet sources
- 11% Publications
- 14% Submitted works (Student Papers)

### Top Sources

The sources with the highest number of matches within the submission. Overlapping sources will not be displayed.

1	Submitted works	Universiti Malaysia Pahang on 2024-06-22	5%
2	Internet	ebin.pub	<1%
3	Publication	Vasile Minea. "Heating and Cooling with Ground-Source Heat Pumps in Cold and ...	<1%
4	Publication	Hanyu Jiang, Shuting Qiu, Bin Ran, Siao Song, Jibo Long. "Energy-saving regulatio...	<1%
5	Publication	Riccardo Conte, Marco Azzolin, Stefano Bernardinello, Davide Del Col. "Experimen...	<1%
6	Submitted works	The Open University of Hong Kong on 2023-04-12	<1%
7	Submitted works	Universiti Malaysia Pahang on 2024-12-12	<1%
8	Submitted works	Universiti Malaysia Pahang on 2024-07-24	<1%
9	Submitted works	Higher Education Commission Pakistan on 2014-01-14	<1%
10	Publication	Paul Tymkow, Savvas Tassou, Maria Kolokotroni, Hussam Jouhara. "Building Servi...	<1%

11	Internet	link.springer.com	<1%
12	Submitted works	VIT University on 2022-06-14	<1%
13	Internet	repository.pnb.ac.id	<1%
14	Publication	Neil Petchers. "Combined Heating, Cooling & Power Handbook - Technologies & A...	<1%
15	Submitted works	University of Leeds on 2013-04-30	<1%
16	Publication	Ashraf Mimi Elsaid. "A novel design, implementation and performance evaluation...	<1%
17	Publication	Keith J. Moss. "Energy Management in Buildings", Routledge, 2006	<1%
18	Internet	pt.scribd.com	<1%
19	Internet	mafiadoc.com	<1%
20	Internet	www.researchgate.net	<1%
21	Submitted works	University of Portsmouth on 2017-09-15	<1%
22	Publication	Watcharapon Watcharajinda, Attakorn Asanakham, Thoranis Deethayat, Tanong...	<1%
23	Publication	Angel Andrade, Juan Zapata-Mina, Alvaro Restrepo. "Exergy and environmental a...	<1%
24	Submitted works	Universiti Teknologi Malaysia on 2011-08-14	<1%

25	Submitted works	Colorado Technical University Online on 2013-04-21	<1%
26	Publication	E.L. Krüger, E.M. González Cruz. "Evolving from an indirect evaporative cooling sy...	<1%
27	Publication	Jing Bai, Huifang Fan, Siqi Cui, Lejian Wang, Siyuan He, Mingzhi Chen, Huifan Zhe...	<1%
28	Publication	Li-Zhi Zhang. "Heat and Mass Transfer in a Total Heat Exchanger: Cross-Corrugat...	<1%
29	Submitted works	University of Duhok on 2022-10-12	<1%
30	Publication	Sachin Dubey, A.M. Guruchethan, Y. Siva Kumar Reddy, M.P. Maiya. "Energy, envir...	<1%
31	Submitted works	University of Wales Swansea on 2024-09-29	<1%
32	Submitted works	Western Governors University on 2014-05-14	<1%
33	Publication	Adal, Anthony. "Gesture Control of a Robotic Arm Using a Microsoft Kinect for De...	<1%
34	Publication	I.M. Rasta, I.N. Suamir. "The role of vegetable oil in water based phase change m...	<1%
35	Submitted works	Middle Technical University on 2023-10-11	<1%
36	Submitted works	National Institute of Technology, Patna on 2016-05-30	<1%
37	Submitted works	University of Sheffield on 2024-05-29	<1%
38	Submitted works	University of Southampton on 2010-10-11	<1%

39	Internet	iacis.org	<1%
40	Internet	patents.justia.com	<1%
41	Internet	sciencedirect.publicaciones.saludcastillayleon.es	<1%
42	Submitted works	Aston University on 2013-05-08	<1%
43	Publication	López-Vidaña Erick César, César-Munguía Ana Lilia, García-Valladares Octavio, Pil...	<1%
44	Submitted works	PSB Academy (ACP eSolutions) on 2023-01-07	<1%
45	Publication	Rim Ben Ali, Souha Bouselmi, Salwa Bouadila, Müslüm Arıcı, Abdelkader Mami. "...	<1%
46	Submitted works	Staffordshire University on 2024-05-13	<1%
47	Submitted works	University of Greenwich on 2024-11-29	<1%
48	Submitted works	University of Sunderland on 2023-10-19	<1%
49	Publication	Wichakan Ketwong, Thoranis Deethayat, Tanongkiat Kiatsiriroat. "Performance e...	<1%
50	Publication	Yabo Wang, Yang Zheng, Xiuzhen Hu, Shengchun Liu, Xueqiang Li, Qihui Wang. "I...	<1%
51	Internet	invotek.ppj.unp.ac.id	<1%
52	Internet	sparcs.info	<1%

53	Internet	vbn.aau.dk	<1%
54	Publication	Amirhossein Ghorbani, Seyed Mohammad Tabatabaei, Hossein Nasiri, Behrang S...	<1%
55	Publication	Behzad Ghobadi, Farshad Kowsary, Farzad Veysi. "Optimization of heat transfer a...	<1%
56	Publication	Elmaghazy, Salah Ahmed Mohamed Elmoselhy. "Analytical Modeling of Fuel Cons...	<1%
57	Publication	H. Maruyama. "Study of magnetic materials using helicity-modulated X-ray magn...	<1%
58	Publication	Juan Francisco Nicolalde, Javier Martinez-Gómez, Víctor H. Guerrero, Andrés Chic...	<1%
59	Publication	Sarah AIOsaimi, Esra Aleisa, Fotouh Al-Ragom. "Techno-environmental assessme...	<1%
60	Publication	Tomasz Suchocki. "Introduction to ORC-VCC Systems: A Review", Energies, 2025	<1%
61	Submitted works	University of Birmingham on 2025-01-30	<1%
62	Submitted works	University of Newcastle on 2006-04-24	<1%
63	Submitted works	University of Sheffield on 2024-03-14	<1%
64	Internet	bmsit.ac.in	<1%
65	Internet	dokumen.pub	<1%
66	Internet	semarakilmu.com.my	<1%

67	Publication	Roslan, Muhammad Amir. "Energy Performance Comparison Between the Variabl...	<1%
68	Submitted works	University of Babylon on 2023-04-28	<1%
69	Publication	Chenjiyu Liang, Xianting Li, Xiangjun Meng, Wenxing Shi, Junqiang Gu, Baolong W...	<1%
70	Submitted works	Military Technological College on 2024-12-23	<1%
71	Submitted works	University of Ulster on 2023-11-07	<1%

ORIGINAL ARTICLE

# Thermodynamic Performance: An Experimental Analysis of a 2.5 kW Split Inverter Air Conditioning Unit with R-410A

I Gede Artha Negara<sup>1\*</sup>, I Wayan Temaja<sup>2</sup>, Luh Putu Ike Midiani<sup>3</sup>, I Dewa Made Cipta Santosa<sup>4</sup>, I Gusti Agung Bagus Wirajati<sup>5</sup>, Made Ery Arsana<sup>6</sup>

<sup>1-6</sup>Department of Mechanical Engineering, Bali State Polytechnic, 80364 Badung, Indonesia

**ABSTRACT** – This research aims to investigate the thermodynamic performance, including temperature differential properties and energy efficiency ratio (EER) of the air conditioning cooling system. A 2.5 kW split inverter air conditioning with R-410A was applied in this research for investigation and integrated with a microcontroller ATmega 2560 for data acquisition. The investigation was carried out between temperature setpoint of 16°C and 20°C. An online psychrometric chart calculator was employed in this research to facilitate the calculation of thermodynamic properties. The results showed that the average temperature differential across all the temperature setpoint was found to be 11°C to 12.89°C. This result indicated an ability to exceed the minimum tolerance allowed for evaporator temperature differential standards. Moreover, the highest result of EER of air conditioning system was found to be 13.87 at a temperature setpoint of 20°C. The research revealed that all temperature setpoint ranging from 16°C to 20°C yielded EER values within the range of 8 to 15, which is widely recognized as the efficient operational range for residential air conditioning applications. In addition, this air conditioning system has better energy efficiency and cost savings over the lifetime of the cooling system. The integration of microcontroller technology in this research facilitated the real-time recording of each investigation parameter. This approach enhanced the efficiency, complexity, and reliability of the experimental investigation of the air conditioning system.

### ARTICLE HISTORY

Received: xxxx  
Revised: xxxx  
Accepted: xxxx  
Published: xxxx

### KEYWORDS

Energy efficiency ratio  
Temperature differential  
Inverter air conditioning  
Thermodynamic

## 1.0 INTRODUCTION

Air conditioning is a trustworthy device to increase human comfort in a compartment or residential purposes. Lately, the demand for air conditioning installations has increased significantly, resulting in an increase in electrical energy consumption [1–6]. Unfortunately, this phenomenon has a negative effect on electrical energy consumption over time. Based on the report [7] one of the biggest contributors to energy consumption in appliances is air conditioning including houses, industrial plants and property. According to the report, roughly 15% of world electrical energy consumption comes from refrigeration and air conditioning systems [8]. However, energy consumption in air conditioning is found to be around 20% in developing countries such as Indonesia [7]. The most familiar unit for air conditioning is vapor-compression refrigeration. This device is most widely used for refrigerators, air conditioners as well as heat pumps [9], [10]. The primary components of the unit are evaporator, compressor, condenser and expansion valve [11–13]. This unit comprises of four processes: 1-2: Compression in a compressor of isentropic. The next process is 2-3: Heat removal in a condenser with isobar. 3-4: Expansion of throttling. 4-1: Thermal absorption in an evaporator with isobar. All components related to vapor-compression refrigeration are steady-flow as a result all processes can be investigated as steady-flow processes [14–17].

In the field of air conditioning technology, the use of inverter technology represents a groundbreaking advancement aimed at addressing the issue of electrical energy consumption [18, 19]. The operational mechanism of an inverter-based air conditioning system differs slightly from that of conventional air conditioning systems. The inverter is able to control the compressor rotation speed thereby reducing the binary on/off cycle [20]. The inverter can regulate the flow rate of refrigerant with evolving the compressor speed [21, 22]. On the other hand, conventional air conditioning is operated generally by fixed-speed. The advantages of inverter air conditioning include the ability to save more energy, enhance temperature regulation, and extend longevity [23, 24]. Moreover, inverter air conditioning systems typically generate less noise compared to traditional air conditioning units. In order to identify the efficiency of an air conditioning cooling system, a thermodynamic parameter is required, known as the energy efficiency ratio (EER). The EER is a measure that compares the rate of heat displacement from the cooled space to the rate of energy consumption by the air conditioning unit [25]. The higher EER indicates the higher energy efficiency of the air conditioning system. Globally, the range of EER for current residential air conditioning systems typically around 8-12 [26]. However, for commercial air conditioning systems the range of EER can be found around 10-16 or even higher. In addition, the EER is commonly utilized as a metric to rate the efficiency of air conditioning systems under specific operating conditions including temperature of indoor and outdoor as well as the relative humidity levels [27].

\*CORRESPONDING AUTHOR | W. Mellon | [waltermellon@ump.edu.my](mailto:waltermellon@ump.edu.my)

In previous study Watcharajinda et al. [28] investigated the effectiveness of an open pond as heat sink for a water-cooled condenser rather than cooling tower. A 3.5 kW air conditioner using R32 and an open pond was utilized in the study. The research shows the capability of employing an open pond as heat sink leveraging evaporative and mechanism of heat exchanger. This research aims to sustain the energy efficiency ratio (EER) of the air conditioner beyond 4.1 by modifying the surface area as well as pond volume ratio. In the research, the air-conditioned chamber temperature was sustained at 23C and a 4 kW of electrical heater was applied as thermostatic control. The next study Andrade et al. [7] conducted an examination of fixed types of air conditioning device under various heat load states using method of EER and cooling seasonal performance factor (Fcsp). Research shows a detailed revision procedures, standard states and the result comparison between two types of air conditioning. This result indicated the method of EER was found to be more accurate when assessed to the Fcsp at real operating states. This result could be beneficial for improve public policies as well as advanced technical planning for developing and designing energy efficiency applications. A study from Conte et al. [25] conducted a research study on the application of low GWP refrigerants as drop alternatives to refrigerant R134a in a compression system with water-to-water vapor. The types of refrigerants employed for investigation are: R513A, R450A, R515B, R516A, R152a, and R1234ze(E). The experimental tests were conducted at full and partial loads with a fixed outlet/inlet temperature of water in the heat exchanger. The experimental data allowed for the analysis of the energy efficiency ratio (EER) for each type of refrigerant respectively. The data compare each refrigerant of R134a: R450A and R152a can reach up to 3.8% and 8.5% higher EER, respectively.

This research study undertook an experimental investigation to evaluate the thermodynamic performance, specifically the energy efficiency ratio (EER) of a split wall inverter air conditioning unit. The experiments were conducted under standardized room heat load conditions. The study utilize microcontroller technology to log data for each of the investigated parameters. The role of the microcontroller was to provide real-time data that is accurate and precise. The tests were carried out with varying air conditioning temperature setpoint. This allowed for a comprehensive analysis of the system's energy efficiency characteristics under different operational conditions. The primary objective of this research study to evaluate the thermodynamic performance, specifically the EER of inverter air conditioning cooling systems under actual operating conditions. Furthermore, this investigation aims to provide comprehensive innovations in microcontroller technology-based instrumentation for data acquisition and analysis. In addition to the EER assessment, this study also examines the range of temperature differential between the evaporator inlet and outlet. This parameter provides valuable insights into the heat transfer characteristics and efficiency of the refrigeration cycle within the air conditioning system. The findings from this study will contribute to a deeper understanding of the energy efficiency characteristics of a split wall inverter air conditioning unit under actual operating conditions.

## 2.0 EXPERIMENTAL AND INSTRUMENTATION SETUP

This research investigation was carried out in the Air Conditioning and Refrigeration Laboratory, Mechanical Engineering Department at Bali State Polytechnic. The air conditioning used in this study was a 2.5 kW split-type inverter air conditioner utilizing R-410A as the working refrigerant. The specific system specifications can be seen in Table 1. These air conditioning is provided with inverter technology which is able to control the compressor speed, making it possible to minimize on/off cycles. This research investigation employed an ATmega 2560 microcontroller as the data logging system. This microcontroller-based setup was utilized to record various system parameters and also provide real-time display of the monitored data. The ATmega 2560 has pins for 54 digital input/output [29, 30], 16 analog inputs and operates at 16 MHz. The technical details of the ATmega 2560 are shown in Table 2 [31]. The experimental setup utilized the latest version of the arduino integrated development environment (IDE) software installed on a personal computer to program the ATmega 2560 microcontroller. The arduino IDE provided a user-friendly platform for the development and implementation of the custom firmware required to operate the data logging and monitoring system based on the ATmega 2560 microcontroller [32]. The k-type thermocouple was applied in this research to measure the temperature of inlet and outlet evaporator. This k-type thermocouple has a measurement range from 0°C to 400°C with a specific error of  $\pm 2^\circ\text{C}$ . In order to ensure the reliability and precision of the temperature measurements, the thermocouples were calibrated against a precision reference thermometer with an uncertainty of  $\pm 0.04^\circ\text{C}$ . This calibration process was conducted to minimize any systematic errors and improve the overall accuracy of the temperature data collected during the experiments.

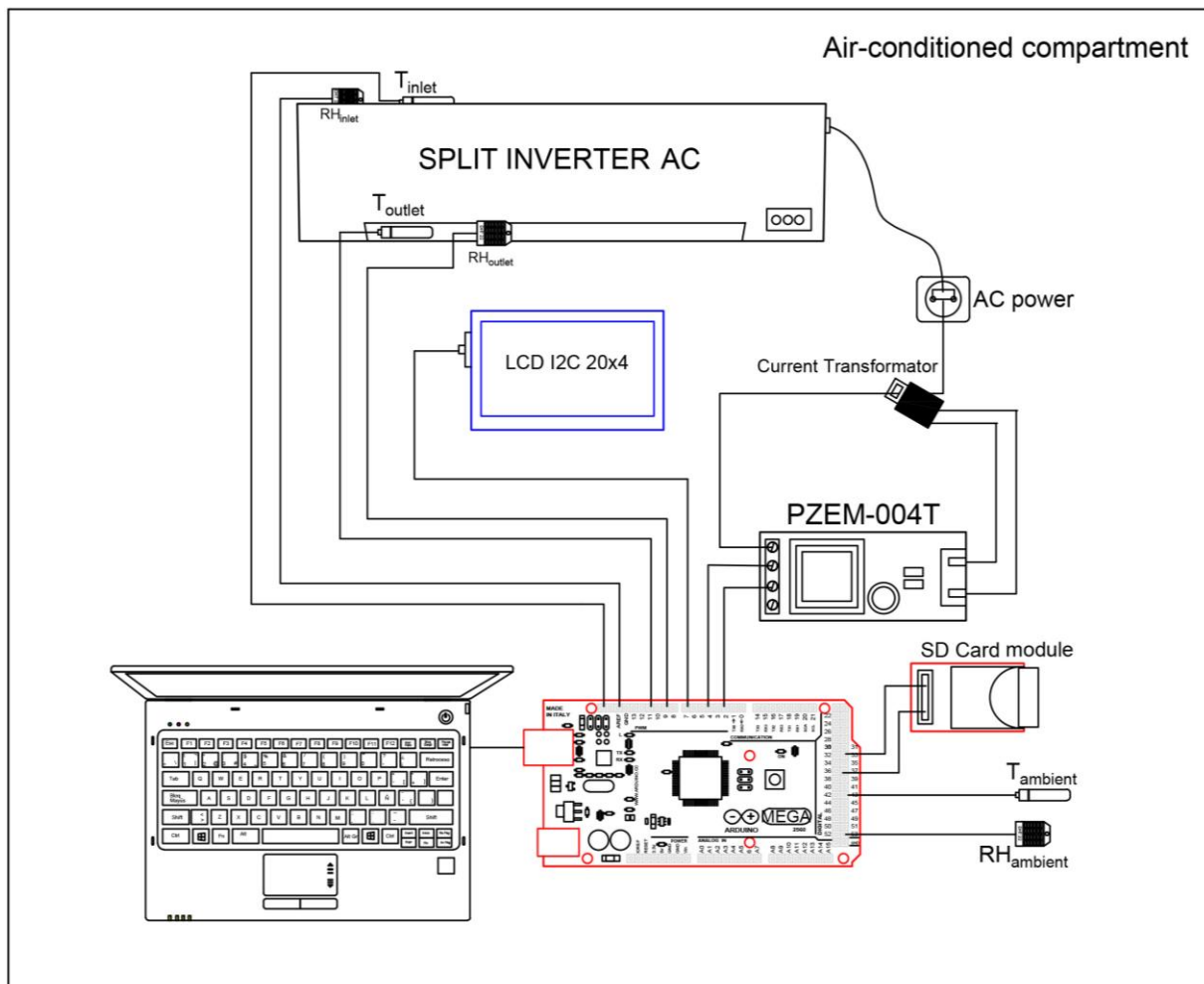
In order to measure relative humidity at the evaporator inlet and outlet, the DHT22 sensor was used in this study with a measurement range of 0% to 100%. Moreover, the PZEM 004-T sensor was utilized in this research to quantify electrical parameters including voltage, current and power consumption. The integration of these specialized sensors into the experimental setup allowed for the simultaneous monitoring of the thermodynamic, psychrometric, and electrical parameters. All instrument accuracies were recorded in Table 3. Digital anemometer was utilized in this research in order to measure the wind speed of air conditioning. An 830-point breadboard was used to connect all electrical components. In order to save the data parameters of an SD card module employed in the installation via jumper cables. A diagram of the experimental setup can be seen in Fig. 1. In addition, online psychrometric diagrams were applied in this research to obtain thermodynamic properties including specific volume, relative humidity, temperature of wet bulb, temperature of dry bulb and enthalpy. These psychrometric diagrams are a crucial component for determining the thermophysical properties of moist air, which is essential for the comprehensive analysis of the air conditioning system's performance. The psychrometric diagram software used was the online interactive psychrometric chart which was established by

FlyCarpet Inc. The ability to seamlessly integrate the psychrometric diagram software into the experimental analysis allowed for the accurate determination of the air properties at various points within the air conditioning system.

23

Table 1. Detailed specification of split inverter air conditioning unit

Parameters	Refrigerant: R-410A	
	Unit	Values
<b>Cooling</b>		
Input power	kW	0.485
Rated current	A	2.7
Maximum power	kW	2.06
Maximum current	A	9.5
Compressor speed range	RPM	600–3600
Capacity	kW	2.5
<b>Heating</b>		
Input power	kW	0.58
Rated current	A	3
Maximum power	kW	2.06
Maximum current	A	9.5
Compressor speed range	RPM	600–3600
Capacity	kW	3.2



64

Figure 1. Schematic illustration of the experimental setup

Table 2. Detailed specification of microcontroller unit

Specification	Details
Microcontroller	ATmega 2560
Voltage of input	7V - 12V
Voltage of operating	5V
Pins of analog input	16
DC current per I/O pin	20 mA
Pins of digital I/O	54
DC current for 3.3V pin	50 mA
Clock speed	16 MHz
EEPROM	4 KB
Flash memory	256 KB (8 KB used by bootloader)
SRAM	8 KB
Communication interfaces	UART (4), I2C, SPI
PWM pins	15 (Pins: 2 to 13, 44 to 46)
USB connection	Type B USB port
ICSP header	Yes
Power jack	Yes
Onboard LED	Yes
Reset button	Yes
Weight	37 grams
Dimensions	101.52 mm x 53.3 mm

Table 3. Instruments accuracy

Parameter	Instrument	Range and unit	Accuracy
Temperature	K-type thermocouple Max6675	0°–400°C	±2°C
Relative humidity	DHT22	0%–100%	±2–5%
Wind speed	Anemometer	0.4–30 m/s	±3.5%
Power	PZEM-004T	0–10 kW	±3%
Current	PZEM-004T	0–100 A	±2%
Voltage	PZEM-004T	80–260 VAC	±1%

Fig. 1 shows both thermocouple and DHT22 sensors positioned on the supply and inlet sides of the evaporators respectively. These sensors are also placed in air-conditioned compartment in order to measure the surrounding ambient air temperature and relative humidity levels. The dry-bulb temperature and relative humidity are utilized to determine thermodynamic properties such as enthalpy, humidity ratio and specific volume through psychrometric diagrams. The PZEM current transformer is connected to the power of the air conditioning system to report electrical parameters. The I2C LCD is connected to the ATmega 2560 via jumper cable to serve as a display during the investigation. Furthermore, an SD card module equipped with memory is linked to the ATmega 2560 for data storage. All instrumentation components are connected to the ATmega 2560 microcontroller and integrate with a PC to receive commands in the format of coding across the arduino IDE application. The investigation was carried out over a duration of two hours, during which the temperature was varied across five distinct setpoints: A (16°C), B (17°C), C (18°C), D (19°C), and E (20°C). In addition, each parameter investigated is plotted on an online psychrometric chart to evaluate the thermodynamic properties of each temperature setpoint variation. This property is used to calculate the energy efficiency ratio (EER) for a 2.5 kW split inverter air conditioning system. The energy efficiency ratio (EER) is a metric that quantifies the performance and cooling efficiency of an air conditioning system. A higher EER value indicates a more energy-efficient AC system. In order to determine the EER value, several equations require including volume flow rate ( $\dot{v}$ ) and mass flow rate ( $\dot{m}$ ) as follows:

$$\dot{V} = V \times A \quad (1)$$

where  $V$  represents the air flow velocity through the evaporator fan (m/s),  $A$  is cross-sectional area of the evaporator fan the area of the evaporator fan ( $\text{m}^2$ ),

$$\dot{m} = \frac{\dot{v}}{v} \quad (2)$$

where  $\dot{V}$  is the volumetric air flow rate ( $\text{m}^3/\text{s}$ ), and  $V$  is the specific volume of air ( $\text{m}^3/\text{kg}$ ). The cooling capacity can be determined by

$$Q_{out} = \dot{m} \times (h_{in} - h_c) \quad (3)$$

where  $\dot{m}$  is the mass flow rate of the air ( $\text{kg}/\text{s}$ ),  $h_{in}$  is the enthalpy of the inlet air ( $\text{kJ}/\text{kg}$ ), and  $h_c$  is the enthalpy of the conditioned (cooled) air ( $\text{kJ}/\text{kg}$ ). The energy efficiency ratio (EER) can be determined by

$$EER = \frac{Q_{out}}{P} \quad (4)$$

where  $Q_{out}$  is the rate of heat removal from the cooled space (kW).  $P$  is the rate of energy consumption by the air conditioning system (W).

### 3.0 RESULTS AND DISCUSSION

#### 3.1 Evaporator Temperature

The variations in the outlet-side evaporator temperature from each temperature setpoint is shown in Fig. 2. From the figure, it can be seen that all temperature setpoint decrease sharply to  $25.75^\circ\text{C}$  at approximately 1500s. Thereafter, the temperatures tend to continue decreasing as they approach  $18^\circ\text{C}$ . The TA temperature was observed to be relatively lower compared to the temperature setpoint. This is due to the TA indicating a temperature of  $16^\circ\text{C}$ , causing the compressor to work harder and operate for a longer duration to achieve the desired cooling effect. The lowest temperature on TA was found  $12.5^\circ\text{C}$  at around 6540s, after which slight fluctuations were observed due to variations in the room thermal load. The results indicate that lower temperature setpoint lead to correspondingly lower temperatures being achieved within the conditioned space [33]. Furthermore, the temperature measured at the TB was observed to be slightly similar to TA. The difference in the temperatures recorded by TA and TB was inclined around  $1^\circ\text{C}$ . The temperatures indicated by the TC and TD were found to be slightly lower in comparison to TA and TB. However, based on the investigation both TC and TD showed similar trends as shown in Fig. 2. The TC and TD were  $17^\circ\text{C}$  at 770s and relatively the same during investigation. In addition, TE was observed to be higher than all temperature setpoint. This is because the compressor operating at a slower pace, which resulted in a slightly higher temperature at the TE compared to the other measurement point [34], [35]. Generally, the outlet-side evaporator temperature shows low values across all the setpoint temperature.

Fig. 3 shows the temperature variation in the inlet-side of the evaporator across different temperature setpoint. From the observation, the temperature TA can be observed to decrease to  $26^\circ\text{C}$  around 1500s and exhibit fluctuations, likely due to the variable room thermal load. The fluctuations observed in the inlet temperature are caused by an unstable and changing thermal load within the room. The behavior is the entry and exit of occupants into the room, which would result in transient changes in the room's thermal load. This effect introduces disturbances to the overall heat transfer process, showing up as fluctuations in the recorded inlet temperature [36]. Additionally, the temperature TB was slightly higher than TA and fluctuations also occurred during the investigation. From the observation, it can be seen that TC, TD, and TE were slightly different. At 4200s, these temperatures were approximately  $27^\circ\text{C}$ . On the other hand, similar fluctuations are observed in TC, TD, and TE as well. In addition, it is evident that the temperature on the outlet-side of the evaporator is directly proportional to the temperature on the inlet-side of the evaporator. However, the temperature at the outlet side of the evaporator is observed to be lower than the corresponding temperature at the inlet side. This is can be attributed to the phenomenon of evaporative cooling, which is the primary function of the evaporator within the refrigeration cycle. As the refrigerant flows through the evaporator, it absorbs heat from the surrounding environment. This heat transfer process facilitates the transformation of the refrigerant from a liquid to a vapor state [23]. The absorption of heat from the room into the evaporator's inlet side provides the necessary latent heat of vaporization for the refrigerant to undergo this phase transition. Consequently, the refrigerant exiting the evaporator outlet side has a lower temperature compared to the inlet side.

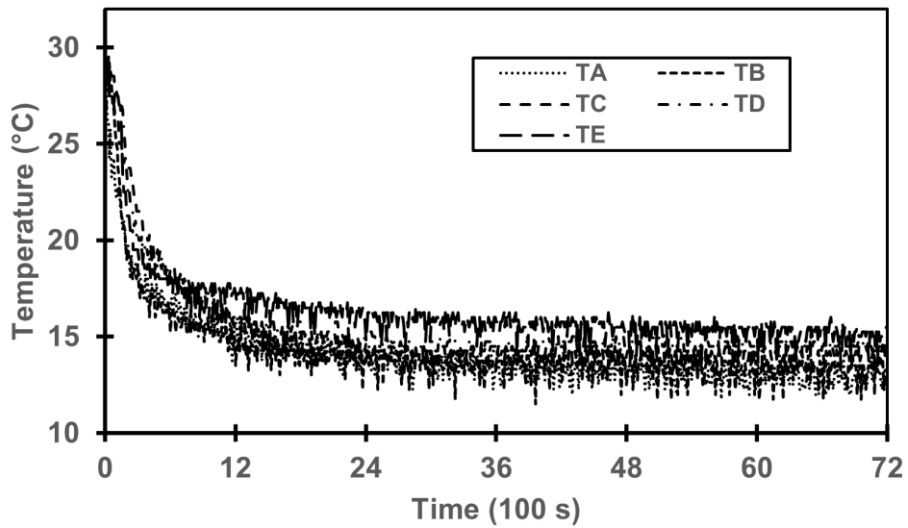


Figure 2. Temperature variation at the evaporator outlet correlated with temperature setpoint

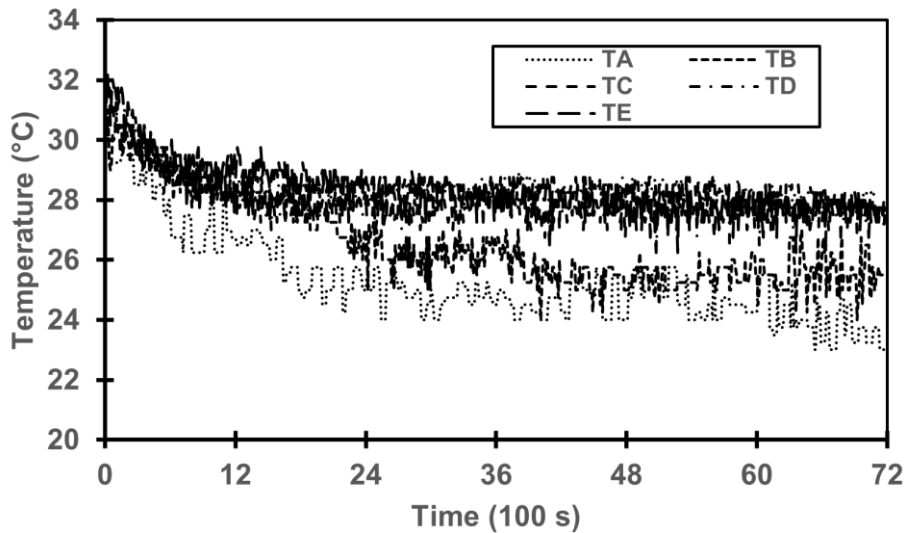


Figure 3. Temperature variation at the evaporator inlet correlated with temperature setpoint

Fig. 4 shows ambient temperature from each temperature setpoint. It is evident that the temperature of TA exhibits the lowest value. This minimum temperature can be attained at approximately 24.5°C. The temperatures of TB and TC were found to be nearly equivalent, with minor variations. Both TB and TC sharply decrease to 26°C at 1110s. Furthermore, the temperature setpoint of TD exhibits a slightly higher than TB and TC. However, it remains relatively lower compared to the temperature of TE. The highest ambient temperature was observed for TE. It is evident that TE represents the highest temperature setpoint, approximately 20°C. This observation is consistent with the expectation that higher temperature setpoint would result in higher ambient temperatures within the conditioned space. Generally, the range of ambient temperatures exhibited across all the evaluated conditions falls within the typical comfort temperature range for Indonesia, a tropical country characterized by high humidity levels. The suitability of these temperature ranges for ensuring thermal comfort in such climatic conditions is a vital factor in the design and operation of air conditioning and refrigeration systems [37].

2

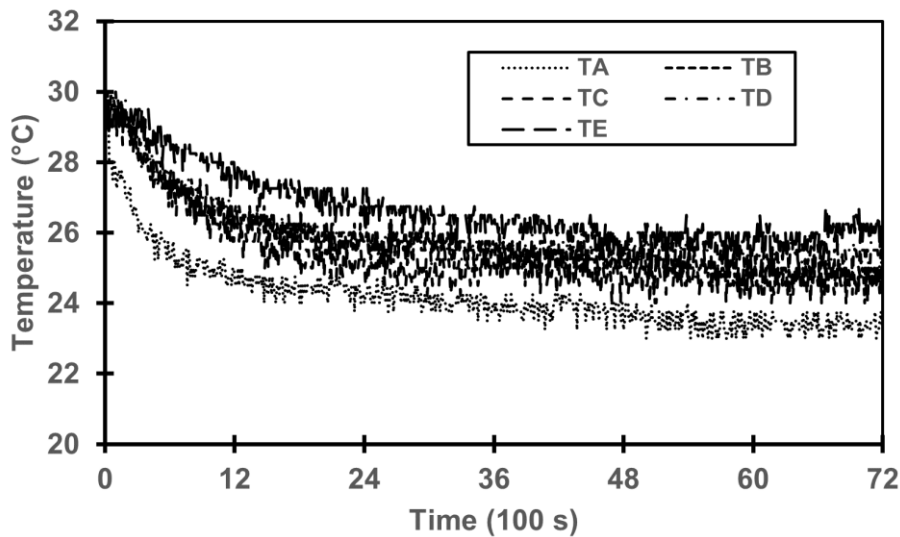


Figure 4. Ambient temperature correlated with temperature setpoint

### 3.2 Temperature Differential

Fig. 5-9 shows the temperature difference between the evaporator's inlet and outlet based on temperature setpoint. From Fig. 5, it is apparent that the temperature differential initially increases significantly, reaching approximately 10°C around 220s for the temperature setpoint of 16°C. The average temperature differential observed during the investigation was 11.19°C. Subsequently, the average temperature differential for the temperature setpoints of 17°C was observed to be 12.31°C as shown in Fig. 6. These results are slightly higher compared to the temperature setpoint of 16°C as shown in Fig. 6. The temperature differential across the evaporator is influenced by several factors, including the cooling load imposed on the system and the prevailing environmental conditions within the conditioned space [38]. These factors can contribute to variations in the heat transfer rates and, consequently, the observed temperature differential. The temperature differential for the temperature setpoint of 18°C can be seen in Fig. 7. From the analysis, the initial surge in temperature differential was lower compared to both temperature setpoint of 16°C and 17°C. However, the average temperature differential for the temperature setpoint of 18°C was found to be 12.76°C. This result is not significantly different from the temperature setpoint of 17°C. Furthermore, the temperature differential for temperature setpoint of 19°C is illustrated in Fig. 8. It can be seen that the average temperature differential exhibits a value of 12.89°C. This result is notably higher than previous temperature setpoint. Moreover, the temperature differential for the final temperature setpoint of 20°C is shown in Fig. 9. Based on the observation, the average temperature differential exhibits a value of 12.13°C. No significant difference was found in the investigation.

Regarding to evaporator temperature differential standards, a minimum tolerance value of 8°C is typically employed as a metric to evaluate the effectiveness of the heat transfer dynamics and the cooling capacity of the evaporator component. The observed average temperature differentials for all the investigated temperature setpoint exceed this minimum tolerance value, indicating that the evaporator is operating within acceptable performance parameters. The temperature differential across the evaporator is directly proportional to the heat transfer rate occurring within the component. A higher temperature differential corresponds to a more significant heat transfer from the conditioned space to the refrigerant flowing through the evaporator. Consequently, a larger temperature differential is indicative of a more effective evaporative cooling process and a greater cooling capacity of the evaporator [21]. The range of average temperature differentials observed in this investigation, spanning from 11.19°C to 12.89°C, suggests that the evaporator is effectively absorbing heat from the surrounding environment and facilitating the transformation of the refrigerant from liquid to vapor. This heat transfer process is essential for providing the desired cooling effect within the conditioned space. In addition, the temperature differential across the evaporator is also closely linked to the comprehensive energy efficiency of the air conditioning system. A higher temperature differential implies that the evaporator can achieve the desired cooling effect with a lower mass flow rate of refrigerant, potentially minimizing the energy consumption related to the compressor work and enhancing the system's overall efficiency.

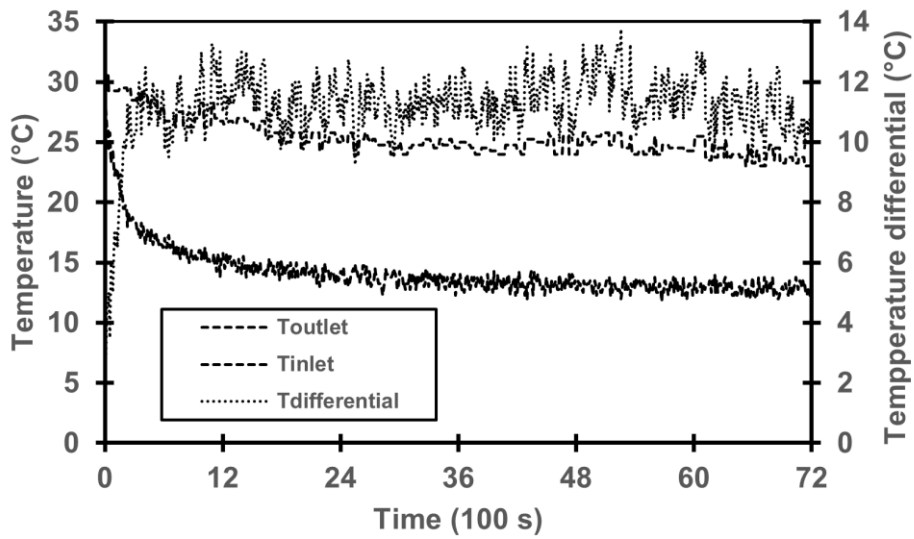


Figure 5. Temperature differential for temperature setpoint of 16°C

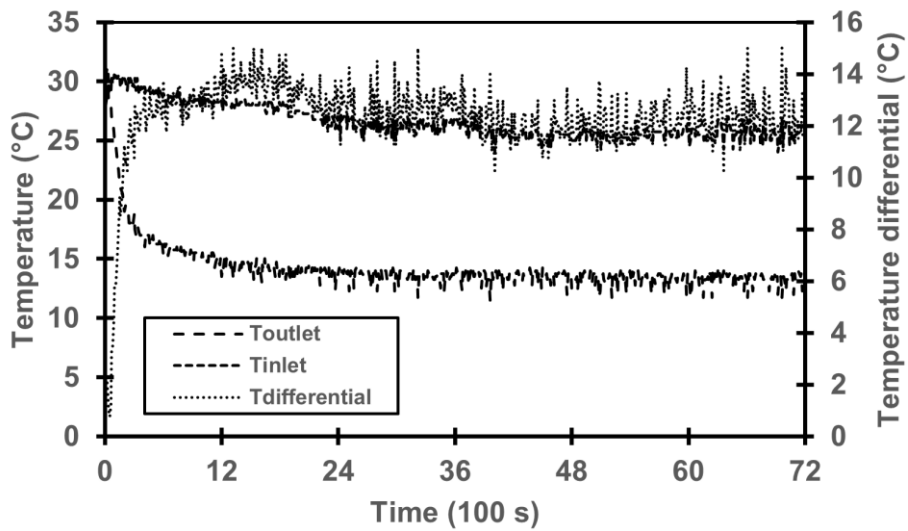


Figure 6. Temperature differential for temperature setpoint of 17°C

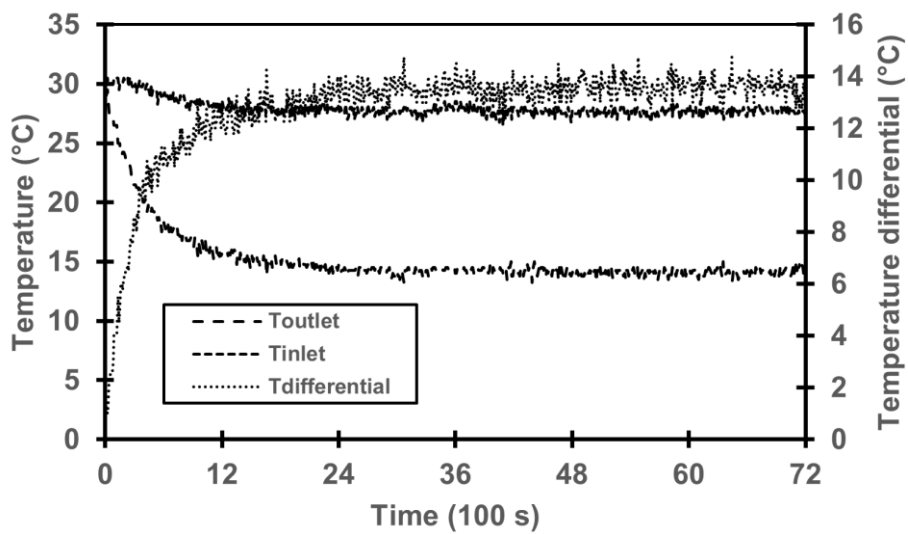


Figure 7. Temperature differential for temperature setpoint of 18°C

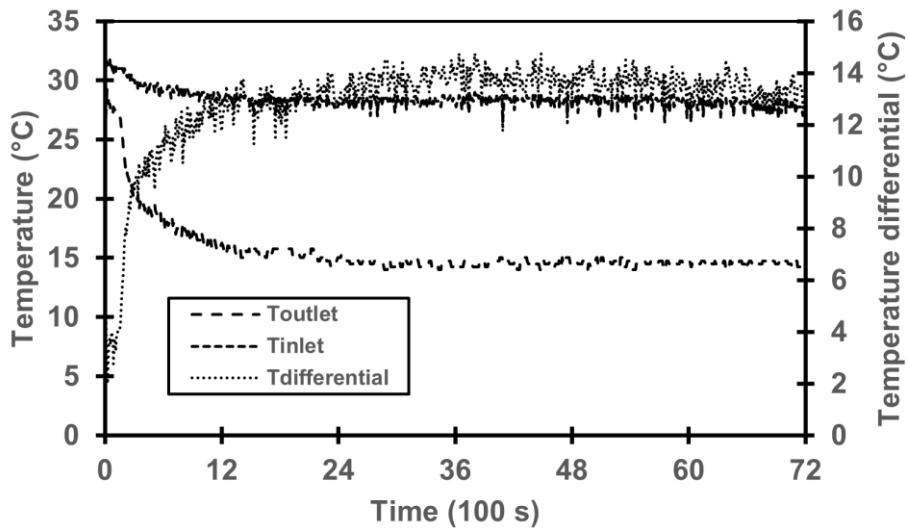


Figure 8. Temperature differential for temperature setpoint of 19°C

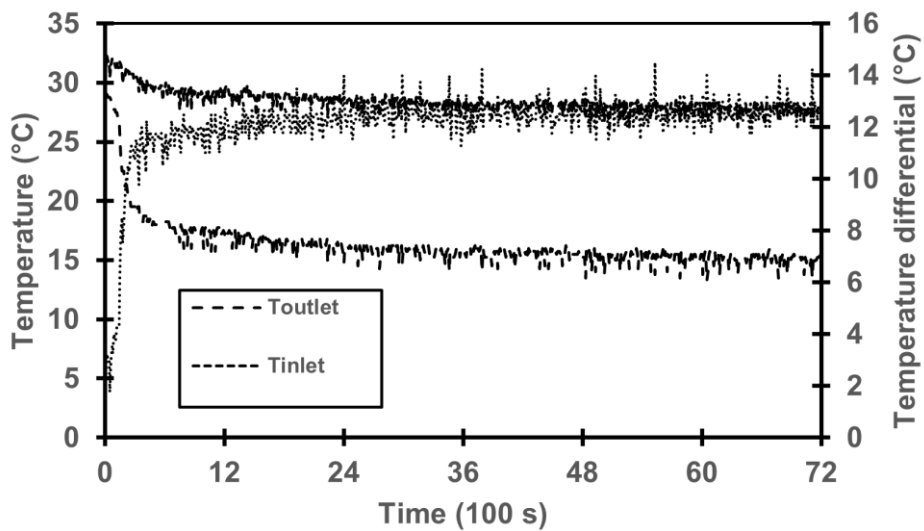


Figure 9. Temperature differential for temperature setpoint of 20°C

### 3.3 Relative Humidity

Fig. 10 shows the relative humidity variation on evaporator outlet-side from each temperature setpoint. The figure shows relative humidity increasing sharply to 90% across all temperature setpoint. This phenomenon can be attributed to the evaporation process, which results in air containing high moisture. When warm air from the room passes through the cold evaporator coil, its temperature drops below the dew point. This causes the water vapor in the air to condense. The evaporation of the refrigerant within the evaporator coils is an endothermic process, meaning that it absorbs latent heat from the surrounding air. This latent heat is required for the phase change of the refrigerant from liquid to vapor. As the refrigerant evaporates, it extracts both sensible heat and latent heat from the air stream. Fig. 4 illustrated the RHA reached 94.2% at 1200s and then remained relatively constant. Moreover, RHA, RHB and RHC tend to be the same with minor fluctuations during investigation. This similarity can be attributed to the comparable evaporation rates and cooling capacities of the evaporator coils at these temperature setpoint. The evaporation process in the evaporator coils absorbs latent heat from the surrounding air, causing the relative humidity to rise [18]. In addition, RHD and RHE were lower, around 89% at 2400s and relatively constant. Based on the observation, the sharp increase in relative humidity is a fundamental characteristic of air conditioning cooling systems and this phenomenon is required for dehumidification as well as effective cooling of space.

10  
32  
18  
14  
46

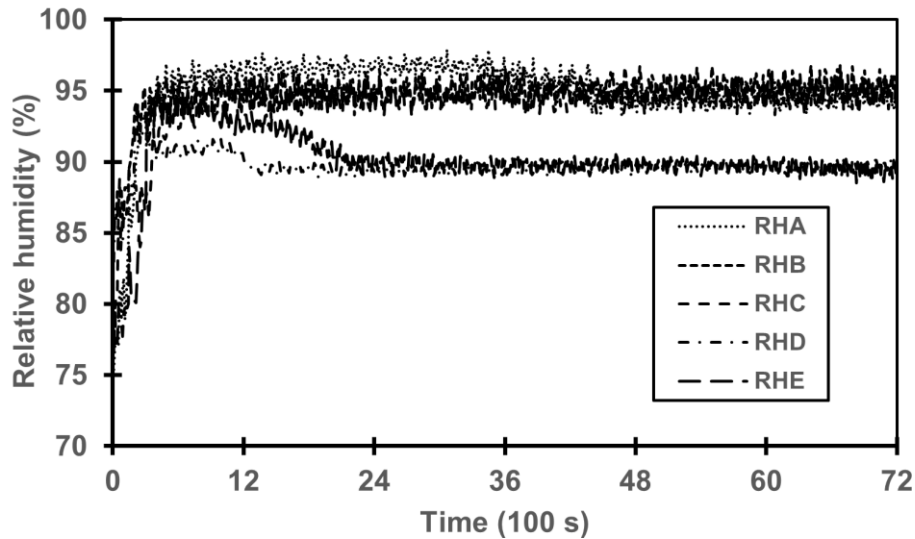


Figure 10. Relative humidity variation at the evaporator outlet correlated with temperature setpoint

Relative humidity variation on the evaporator inlet-side from each temperature setpoint can be shown in Fig. 11. From Fig. 11, all temperature setpoint demonstrated a rapid reduction in relative humidity. This is because the initial moisture content of the air was too high and the temperature was significantly different between the inlet and outlet evaporator sides. When the air passes over the evaporator coils, the condensation process occurs rapidly, resulting in a significant decrease in relative humidity. From the observation, both RHA and RHB showed a similar trend of reduction to 60% at 2270s and then tended to approach each other. Similar results were found in RHC and RHD. At about 3040s both RHC and RHD were 60%. During investigation, the relative humidity was found to be decreasing slowly due to the reducing temperature difference and the decreasing moisture content of the air. The higher the temperature setpoint, the higher the initial relative humidity, as the warmer air held more moisture. Nevertheless, as the air travels through the evaporator, the relative humidity shows a similar final result which indicates the air has reached the state of dehumidification [39].

Fig. 12 shows the ambient relative humidity from each temperature setpoint. It can be seen, that all the variables show a high relative humidity around 75% at 0s and then relatively decrease. When the air conditioning starts to operate, the relative humidity levels indicate a gradual decrease across all temperature setpoints. RHA was found to be 62.7% at 2400s, 65.1% for RHB and 64.2% for RHC. Furthermore, RHD and RHE show 65% and 65.5% respectively at 2400s. The rate of reduction in relative humidity is higher for lower temperature setpoint. From Fig. 6, RHA shows the fastest reduction while RHE indicates the slowest reduction. At lower temperature setpoint, the air conditioning system must remove a greater quantity of sensible heat from the air to achieve the desired cooling effect [20]. This process involves the expansion of the refrigerant gas, which absorbs heat from the surrounding air, resulting in a decrease in air temperature. As the air temperature decreases, its capacity to hold water vapor also decreases, according to the principles of psychrometrics. When the air temperature falls below the dew point, excess water vapor in the air condenses on the cooling coils of the air conditioning unit, thereby reducing the moisture content and, consequently, the relative humidity of the air. In addition, the lowest relative humidity can be reached is about 58%. After around 3600s, the relative humidity was stabilize and fluctuated around specific levels. The lower temperature setpoint indicated the more effective dehumidification.

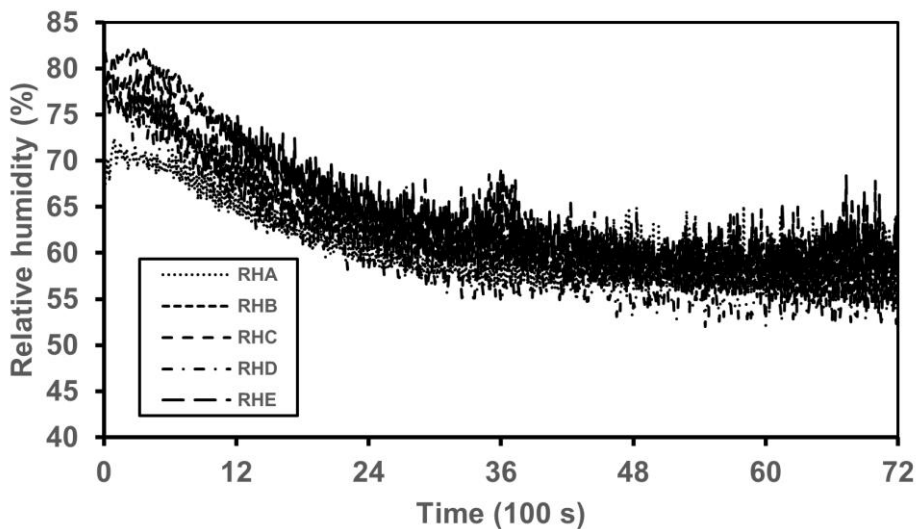


Figure 11. Relative humidity variation at the evaporator inlet correlated with temperature setpoint

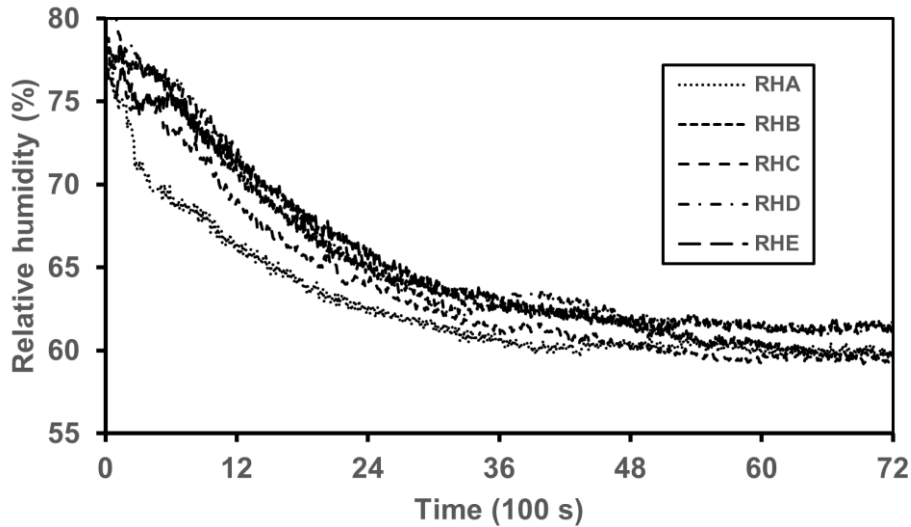


Figure 12. Ambient temperature correlated with temperature setpoint

### 3.4 Psychrometric Analysis

In order to determine thermodynamic properties, an online psychrometric chart calculator is used to determine parameters including enthalpy, specific volume, humidity ratio, specific heat, and dew point temperature. Table 4 shows the thermodynamic properties from each temperature setpoint. The psychrometric chart cycle for each temperature setpoint is shown in Fig. 13-17. These psychrometric charts are displayed in imperial units. All temperature results have been converted to imperial units to facilitate plotting on the psychrometric charts. The average inlet temperature for the setpoint of 16°C was found to be 25.29°C and 60.89% for the average of relative humidity. Subsequently, the average inlet temperature for the setpoint of 17°C was 26.55°C and the average relative humidity was 62.32%. At setpoint 18°C, the average temperature was 27.94°C and the average relative humidity inlet was 64.8%. The average inlet temperature for the setpoint 19°C was 28.4°C and 60.58% for the relative humidity. At setpoint 20°C the average inlet temperature and relative humidity was 28.4°C and 64.7% respectively. The average outlet temperature for the 16°C setpoint was found to be 14.09°C, and the average relative humidity was 95.08%. For the 17°C setpoint, the average temperature was 14.23°C, and the average relative humidity was 94.71%. At the 18°C setpoint, the average temperature was 15.18°C, and the average relative humidity was 94.18%. The average outlet temperature for the 19°C setpoint was 15.50°C, and the average relative humidity was 89.65%. For the 20°C setpoint, the average temperature was 16.26°C, and the average relative humidity was 90.16%. In addition, the overall ambient temperature and relative humidity for the setpoint of 16°C were observed to be 24.19°C and 62.69%, respectively. At the temperature setpoint of 17°C, the average ambient temperature and relative humidity were 25.73°C and 64.8%, respectively. The average ambient temperature for the setpoint of 18°C was 25.28°C, and the average relative humidity was 63.71%. At the setpoint of 19°C, the average ambient temperature was 25.94°C, and the average relative humidity was 65.46%. Additionally, the average ambient temperature and relative humidity for the setpoint of 20°C were observed to be 26.66°C and 65.34%, respectively. The properties of air at the evaporator inlet and outlet sides, as well as the ambient conditions for each temperature setpoint, can be seen in Figs. 18-20.

Table 4. The thermodynamic properties of the air are dependent on the specified temperature setpoint

Temperature setpoint (°C)	Relative Humidity (%)	Humidity Ratio (g/kg)	Specific Heat (kJ/kg.K)	Temperature Dew Point (°C)	Enthalpy (kJ/kg)	Specific Volume (m <sup>3</sup> /kg)
Inlet 16	60.89	12.34	1.023	17.20	56.862	0.862
Inlet 17	62.32	13.635	1.025	18.762	61.460	0.868
Inlet 18	64.8	15.424	1.027	20.703	67.458	0.874
Inlet 19	60.58	15.424	1.026	20.703	67.458	0.874
Inlet 20	64.7	15.829	1.027	21.113	68.965	0.876
Outlet 16	95.08	9.567	1.018	13.316	38.343	0.826
Outlet 17	94.71	9.618	1.018	13.395	38.614	0.827
Outlet 18	94.18	10.178	1.019	14.253	41.002	0.830

Outlet 19	89.65	89.650	1.018	13.810	40.589	0.831
Outlet 20	90.16	90.160	1.019	14.647	42.786	0.834
Ambient 16	62.69	11.888	1.023	16.631	54.582	0.858
Ambient 17	64.8	13.504	1.024	18.611	60.282	0.865
Ambient 18	63.71	12.915	1.024	17.915	58.318	0.863
Ambient 19	65.46	13.819	1.025	18.972	61.301	0.866
Ambient 20	65.34	14.406	1.025	19.625	63.539	0.869

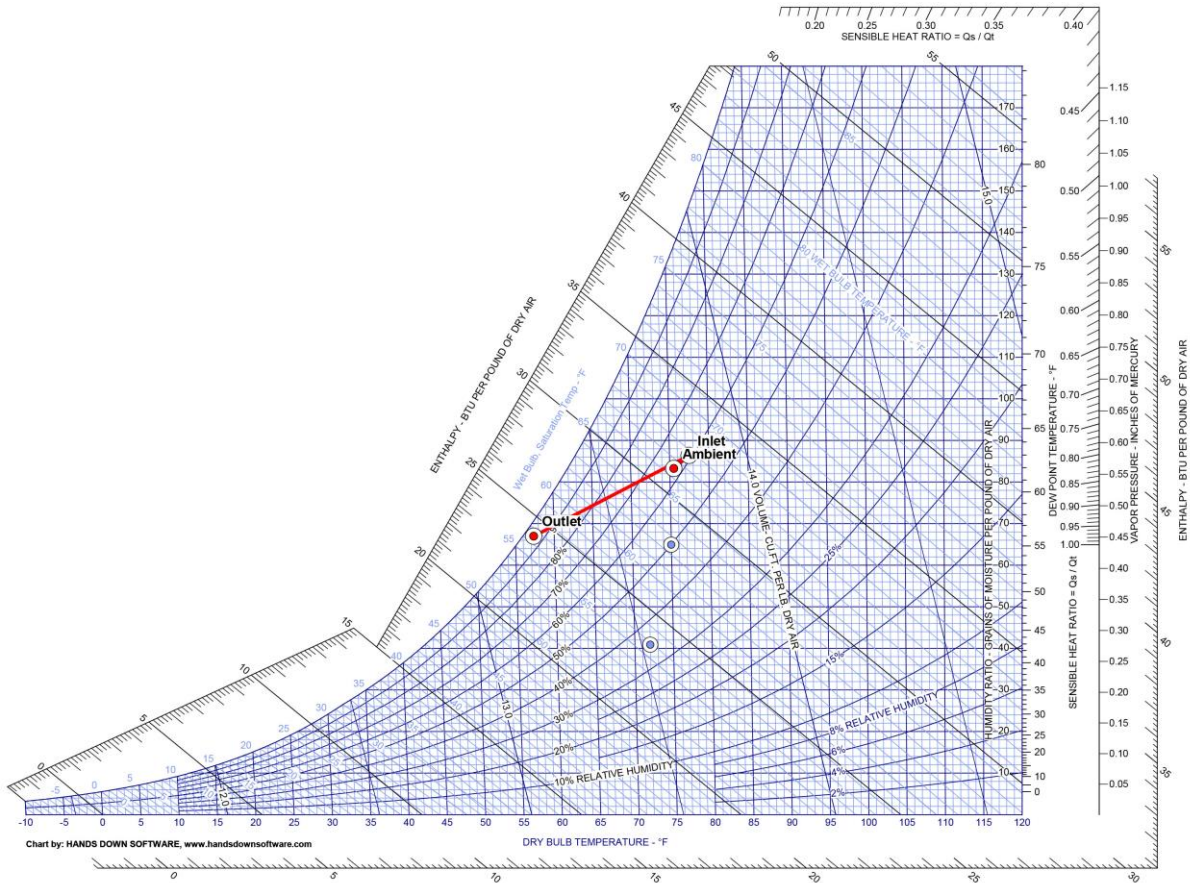


Figure 13. Psychrometric chart cycle related to a temperature setpoint of 16°C

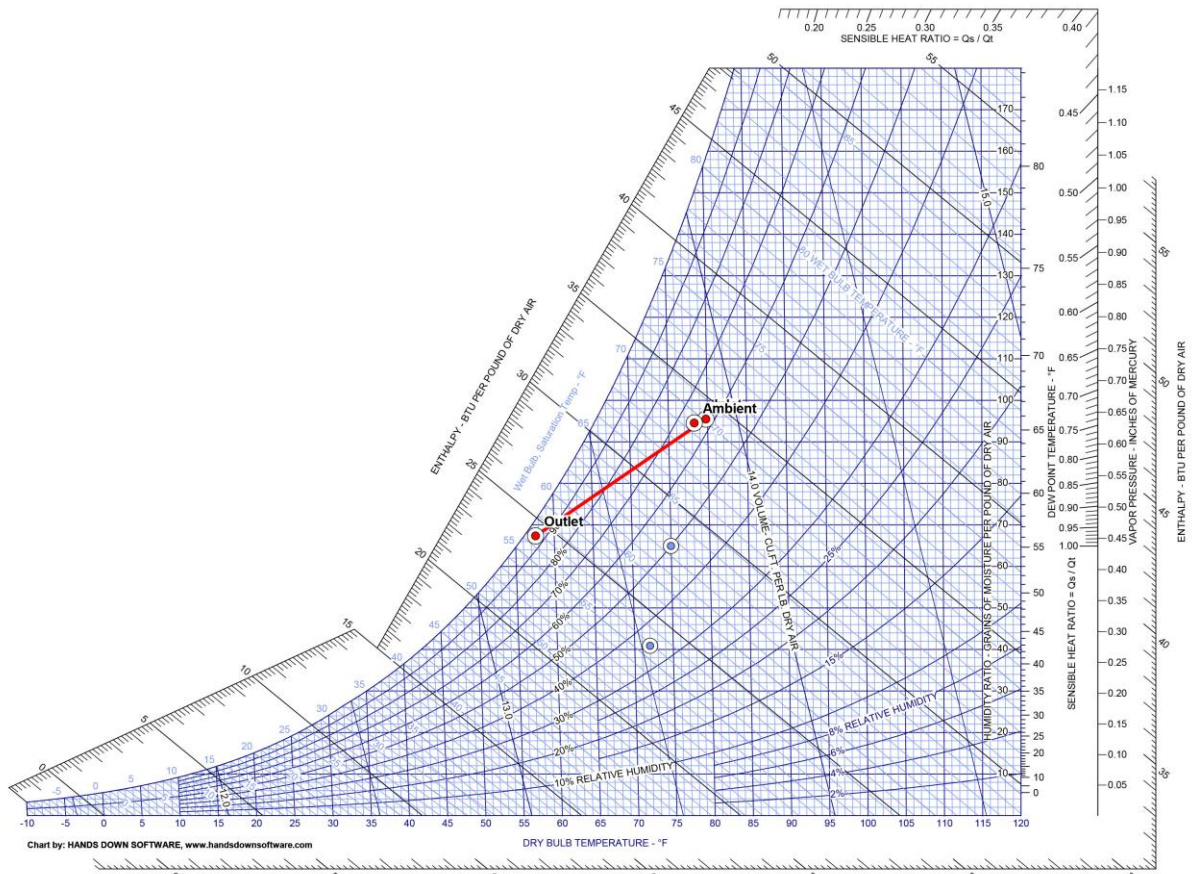


Figure 14. Psychrometric chart cycle related to a temperature setpoint of 17°C

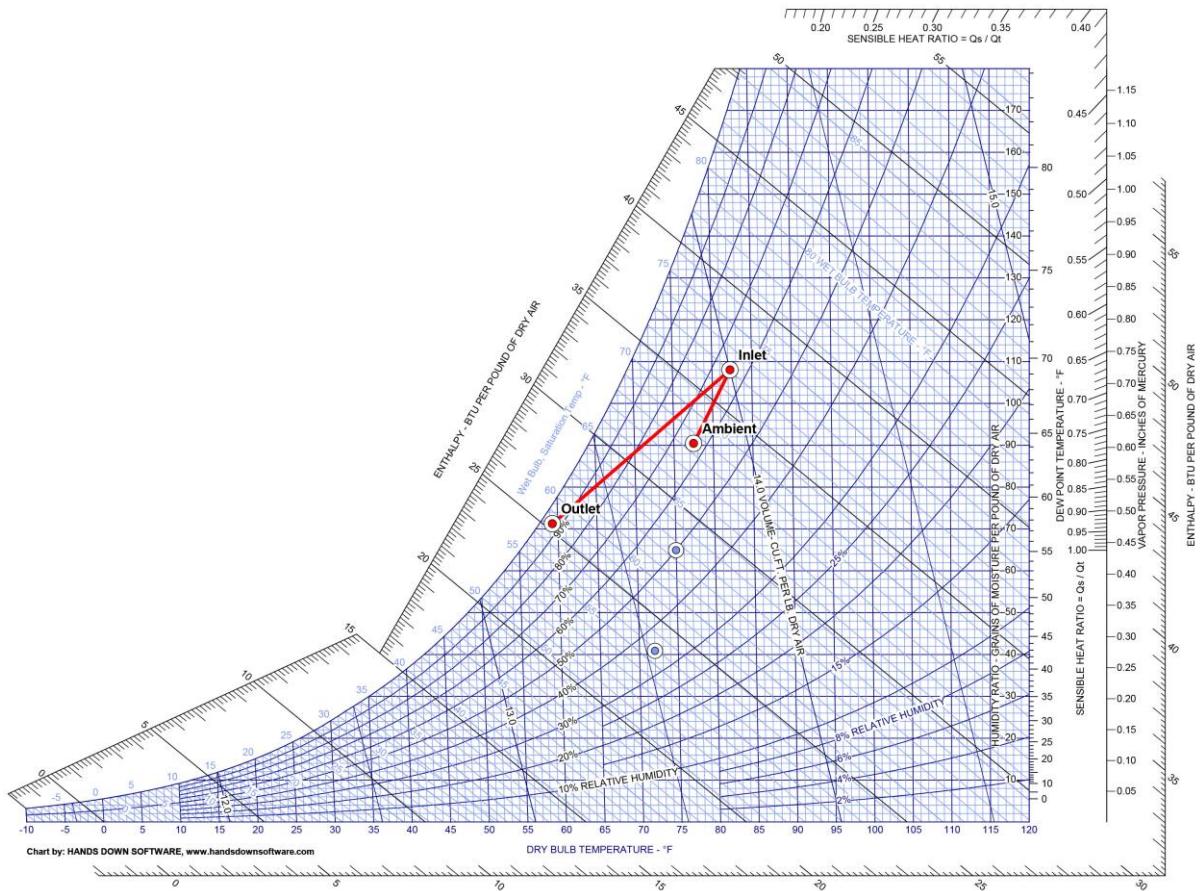


Figure 15. Psychrometric chart cycle related to a temperature setpoint of 18°C

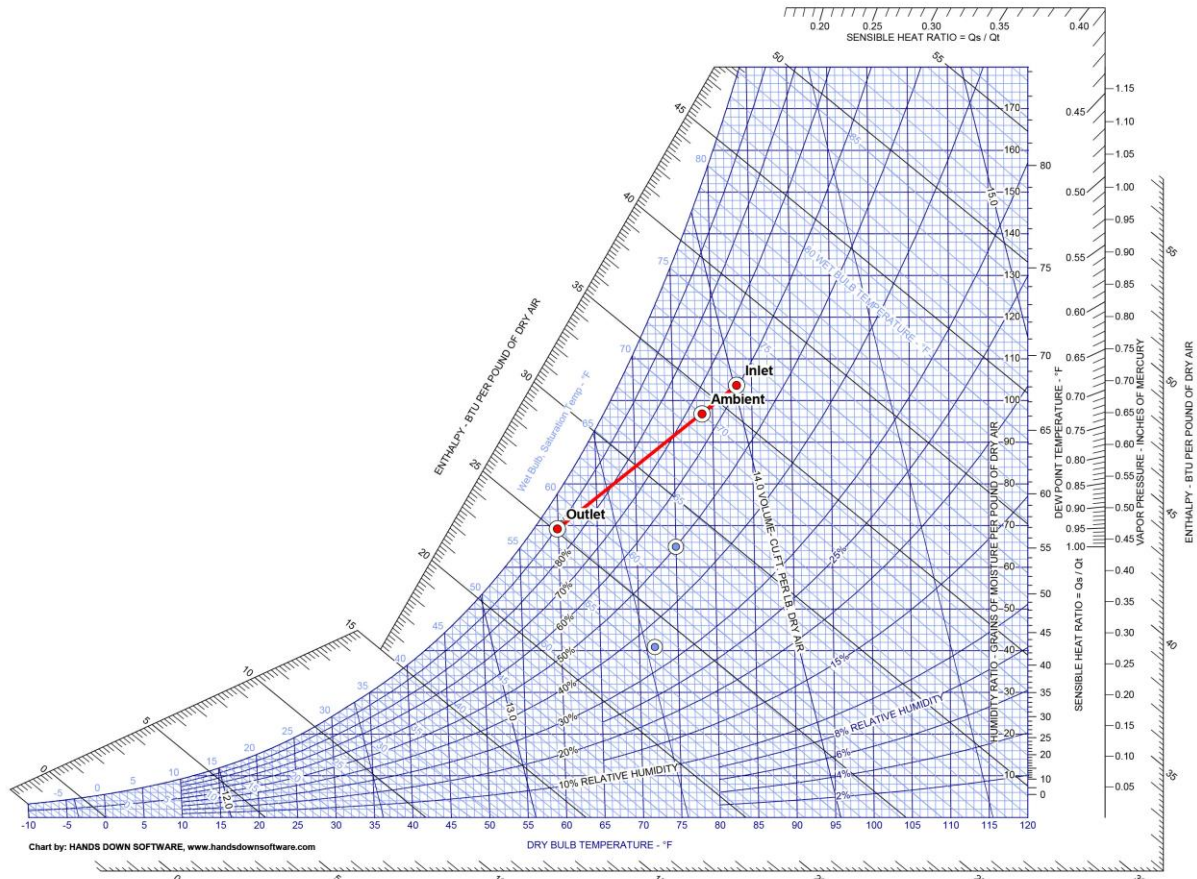


Figure 16. Psychrometric chart cycle related to a temperature setpoint of 19°C

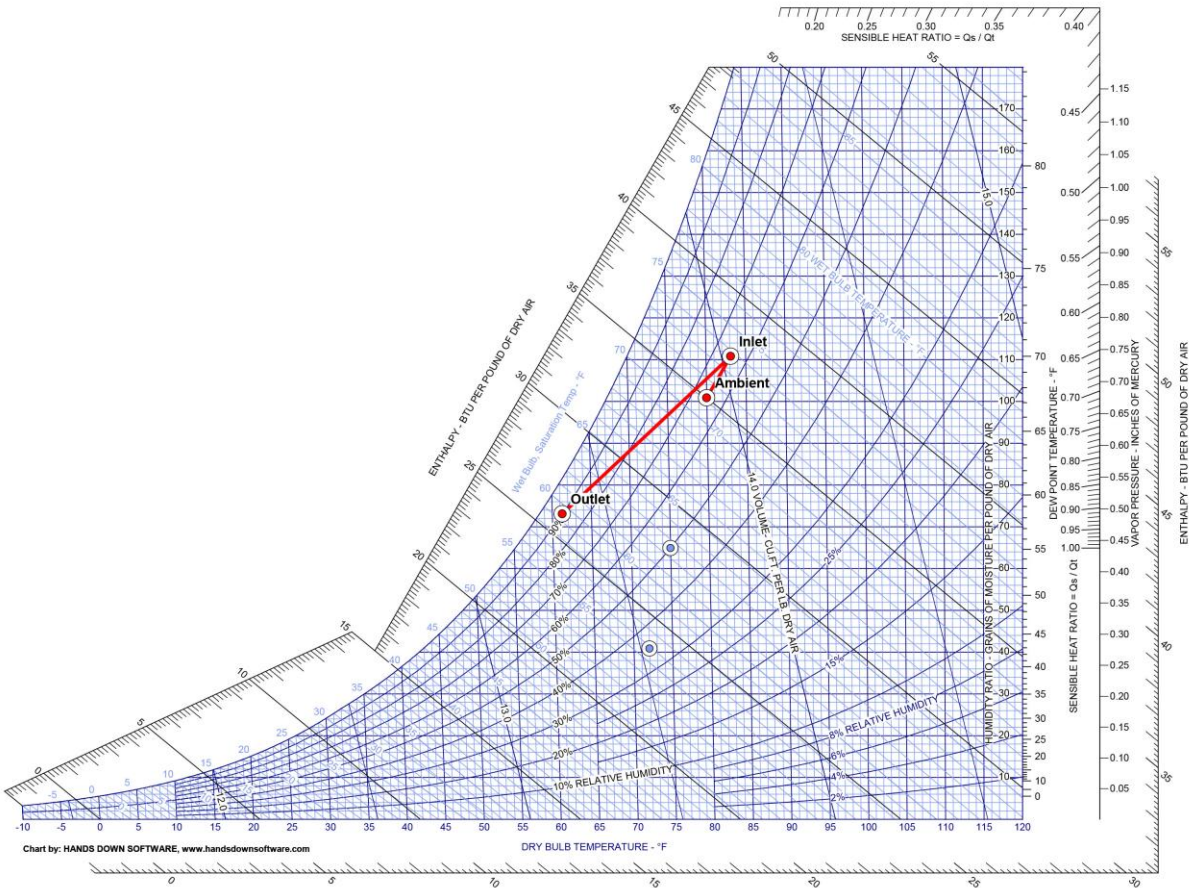


Figure 17. Psychrometric chart cycle related to a temperature setpoint of 20°C

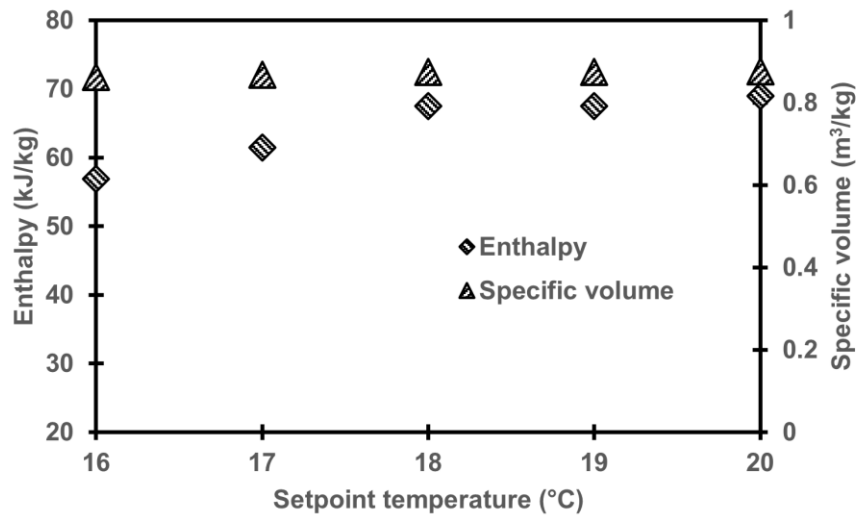


Figure 18. Air properties at the inlet side of the evaporator

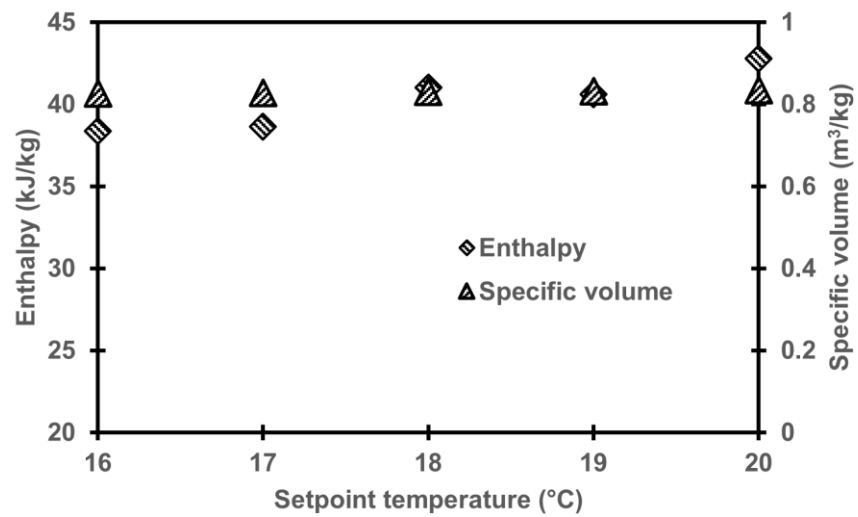


Figure 19. Air properties at the outlet side of the evaporator

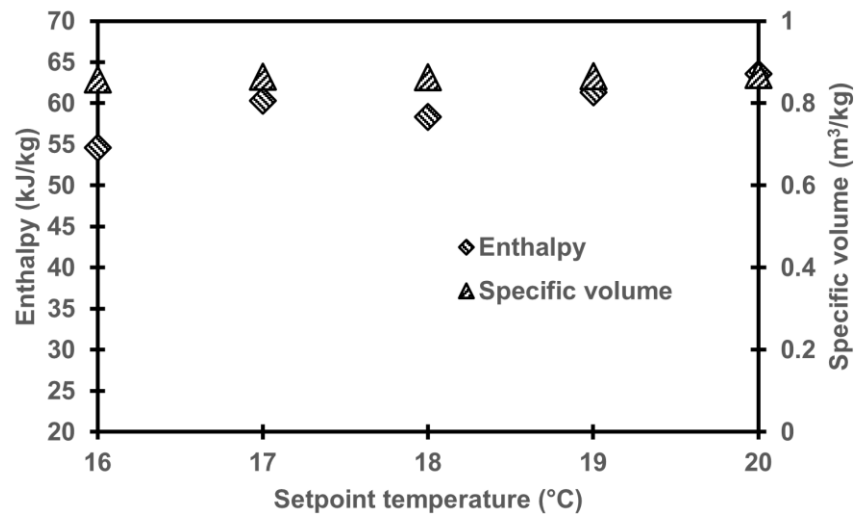


Figure 20. Air properties at ambient conditions

### 3.5 Electrical Characteristic

Fig. 21 shows the voltage from each temperature setpoint. The fluctuations were found in the voltage levels as the air conditioning cooling system begins with frequency and varying degrees of intensity depending on the temperature setpoint. These fluctuations are caused by the cooling load on the air conditioning device which maintains the indoor

temperature and relative humidity. From Fig. 21, it can be seen that the VA and VB show more frequent and larger voltage fluctuations from the baseline level. This behavior is attributable to the increased cooling load placed on the air conditioning system at these lower temperature setpoint, requiring more frequent compressor cycling to remove heat from the indoor environment. In addition, some of the voltage fluctuations evident in the profiles likely correspond to the intermittent operation of auxiliary components within the air conditioning unit. These include fans used to circulate air over the evaporator and condenser coils, as well as defrost cycles implemented to prevent ice buildup on the evaporator during periods of high humidity [40].

Fig. 22 shows the electric current from each temperature setpoint. The sharp increase was found in current across all the temperature setpoints due to the initial current required to operate the compressor and supplementary components of the air conditioning. During the initial phase, observed at approximately 100s, the current reaches a peak value of 1.4A for all temperature setpoint. This surge in current is attributable to the high inrush current demanded by the air conditioning compressor and auxiliary components, such as fans and control circuitry, during the startup sequence. Furthermore, the current profiles exhibit a gradual increase, eventually stabilizing at approximately 2.30A around 400s. This sustained current level corresponds to the steady-state operating condition of the air conditioning system, where the compressor and associated components are actively engaged in maintaining the desired indoor temperature and humidity levels. The lower temperature setpoint generally exhibit higher steady-state current demands compared to higher temperature setpoint. This behavior is expected, as lower temperature setpoint impose a greater cooling load on the air conditioning unit, necessitating increased energy consumption to remove the additional heat from the indoor environment. Despite the overall stability of the current profiles during steady-state operation, minor fluctuations are observed across all temperature setpoint. These fluctuations can be attributed to variations in room conditions [41], such as changes in ambient temperature, humidity levels, or occupancy patterns, which influence the cooling load and subsequently impact the energy consumption of the air conditioning system.

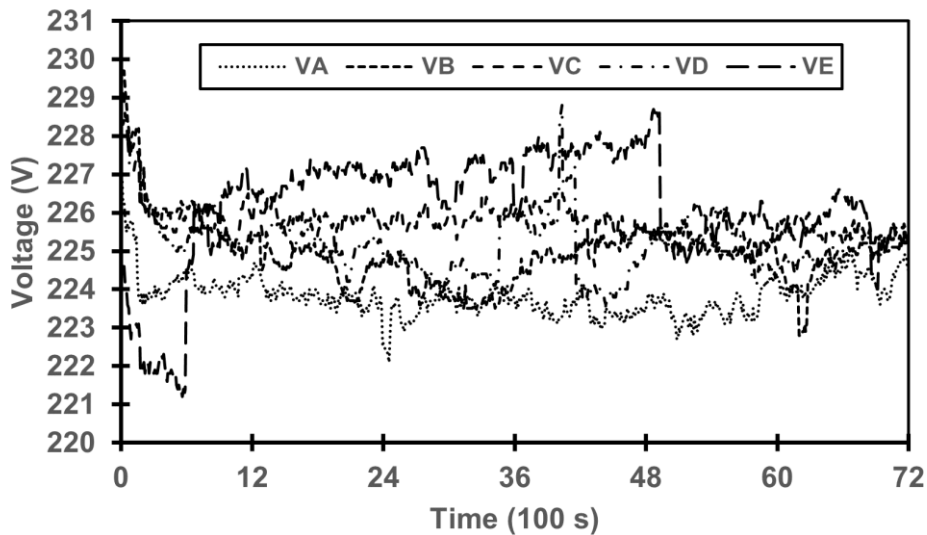


Figure 21. Voltage variation correlated with temperature setpoint

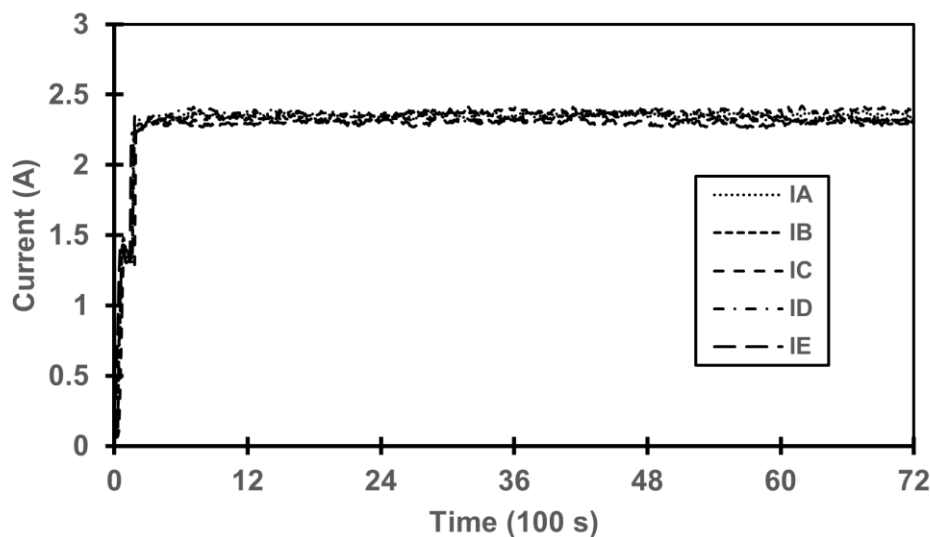


Figure 22. Electric current variation correlated with temperature setpoint

Fig. 23 shows the power consumption from each temperature setpoint. At approximately 600s, a significant increase in power consumption is observed, reaching a peak value of approximately 400w for all temperature setpoint. This surge in power demand is directly attributed to the increased workload placed on the compressor during the initial cooling phase, as it expends substantial energy to remove heat from the indoor environment and achieve the desired temperature setpoint. Subsequent to this initial transient period, the power consumption profiles exhibit minor fluctuations around a sustained level, which varies with the respective temperature setpoint. These fluctuations are indicative of the dynamic nature of the cooling process, where the air conditioning unit modulates its power consumption in response to changes in the thermal load, ambient conditions, and other external factors affecting the cooling demand. From Fig. 21, it can be observed the direct proportionality between the power consumption and the electric current drawn by the air conditioning unit. As the current increases, a corresponding rise in power consumption is observed, reflecting the fundamental relationship between electrical power, voltage, and current in accordance with Ohm's law [42]. Furthermore, it can be seen an inverse relationship between the temperature setpoint and the steady-state power consumption levels. As the temperature setpoint increases from PA to PE, the power consumption decreases accordingly. This behavior is expected, as higher temperature setpoint require a reduced cooling effort from the air conditioning unit, thereby lowering the energy demand and associated power consumption [43]. In addition, the power consumption of an air conditioning system is influenced by various factors beyond the temperature setpoint. These include the thermal load imposed by external conditions, such as ambient temperature, solar radiation, and occupancy levels, as well as the efficiency and performance characteristics of the air conditioning unit itself.

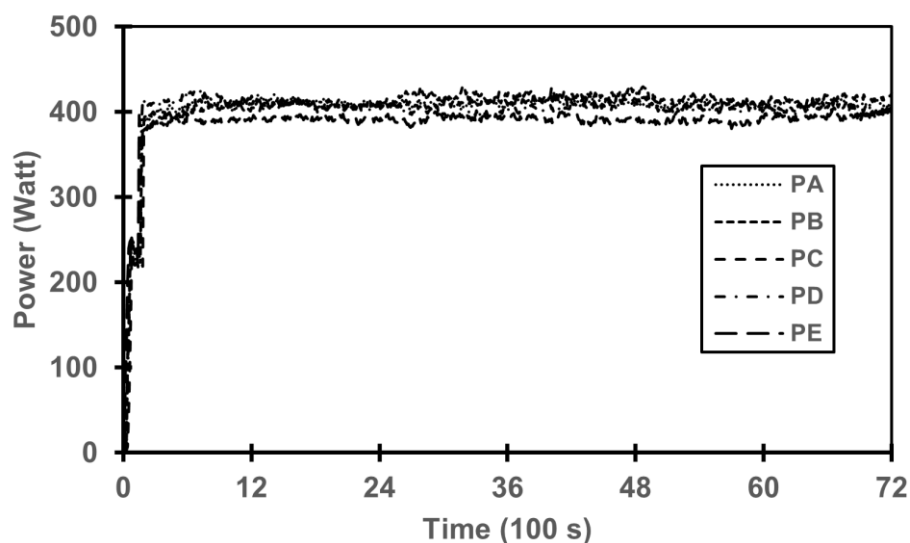


Figure 23. Power consumption variation correlated with temperature setpoint

### 3.6 Energy Efficiency Ratio (EER)

Fig. 24 shows the thermodynamic properties energy efficiency ratio (EER) from each temperature setpoint. It can be known that the EER gradually increases proportionally with temperature elevation. At temperature setpoint 16°C, the observed EER was 10.25 and 10.51 for temperature setpoint 17°C. Both temperature setpoint 16°C and 17°C almost show no significant difference. The air conditioning cooling system works harder to maintain the desired temperature difference between indoor and outdoor environments. This phenomenon causes a lower EER value. Subsequently, temperature setpoint 18°C and 19°C show a slight increase compared to temperature setpoint 16°C and 17°C, which were 11.74 and 12.24 respectively. This improvement in efficiency can be explained by the reduced temperature difference between the indoor and outdoor environments, which results in a lower cooling demand and, consequently, a more efficient operation of the air conditioning unit [44]. However, the most significant enhancement in EER is observed at the highest temperature setpoint of 20°C, where the EER reaches a value of 13.87. This substantial increase in efficiency can be attributed to the further reduction in the cooling load, as the temperature variation across indoor and outdoor conditions becomes smaller. At these higher temperature setpoint, the air conditioning system can operate more efficiently, as the compressor and associated components are subjected to lower thermal stresses and energy demands. Moreover, all the temperature setpoint investigated in this study exhibit EER values within the range of 8 to 15, which is generally considered an efficient operating range for residential air conditioning systems [28]. This indicates that the air conditioning unit employed in this study can be categorized as an efficient cooling system, capable of providing effective cooling while minimizing energy consumption. In addition, the relationship between temperature setpoint and EER can be explained by the fundamental principles of thermodynamics and the refrigeration cycle using vapor compression employed in air conditioning systems. As the temperature setpoint increases, the energy required to attain the desired cooling effect, it reduces, leading to a higher EER. This is because the compressor needs to work less to maintain a smaller temperature differential, resulting in lower energy consumption while still providing adequate cooling capacity.

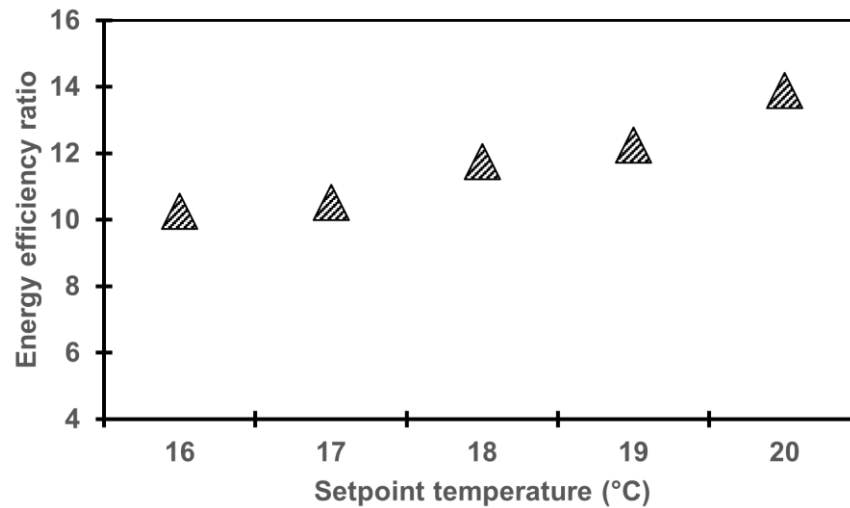


Figure 24. Energy efficiency ratio correlated with temperature setpoint

## 4.0 CONCLUSIONS

The cooling performance coefficient of split inverter air conditioning depends on variation in temperature setpoint, which has been investigated in this study. The highest EER value was found at a temperature setpoint of 20°C, which is 13.87. The higher the temperature setpoint, the higher the EER value of split inverter air conditioning. All temperature setpoint ranging from 16°C to 20°C yielded EER values within the range of 8 to 15, which is considered efficient for residential air conditioning applications. The split inverter air conditioning system employed in this study was deemed efficient for residential use. This finding highlights the suitability of split inverter air conditioning systems for residential cooling purposes, as they can maintain desirable indoor temperatures while operating within the bounds of energy efficiency. In addition, the temperature differential from the inlet to the outlet of the evaporator has a good differential for the standard differential tolerance of air conditioning. The investigation revealed an average temperature differential of 11.19°C to 12.89°C across all temperature setpoint, indicating the evaporator's efficacy in absorbing heat for the liquid refrigerant to undergo vapor evaporation. The utilization of microcontroller technology in this study facilitated the real-time recording of each investigation parameter, thereby enhancing the efficiency, sophistication, and reliability of the experimental process. Moreover, microcontrollers are programmable, allowing for the implementation of customized algorithms and data processing routines. This capability enabled real-time data processing, analysis, and visualization, eliminating the need for time-consuming post-processing steps and providing immediate feedback on the system's behavior. By leveraging the capabilities of microcontroller technology, this study established an automated and streamlined approach to cooling system investigations. The real-time data acquisition, processing, and analysis capabilities provided by microcontrollers not only enhanced the efficiency of the experimental process but also minimized the potential for human error, enhancing the consistency and accuracy of the findings.

## 5.0 ACKNOWLEDGEMENT

The authors acknowledge the financial support received from P3M of Bali State Polytechnic Indonesia.

## 6.0 REFERENCES

- [1] H. Jiang, S. Qiu, B. Ran, S. Song, and J. Long, "Energy-saving regulation methods and energy consumption characteristics of office air-conditioning loads in hot summer and cold winter areas," *Energy Built Environ.*, no. February, 2024, doi: 10.1016/j.enbenv.2024.04.009.
- [2] M. Dai, H. Li, X. Li, and S. Wang, "Reconfigurable supply-based feedback control for enhanced energy flexibility of air-conditioning systems facilitating grid-interactive buildings," *Adv. Appl. Energy*, vol. 14, no. April, p. 100176, 2024, doi: 10.1016/j.adapen.2024.100176.
- [3] T. Randazzo, F. Pavanello, and E. De Cian, "Adaptation to climate change: Air-conditioning and the role of remittances," *J. Environ. Econ. Manage.*, vol. 120, no. February 2022, p. 102818, 2023, doi: 10.1016/j.jeem.2023.102818.
- [4] I. M. Rasta and I. N. Suamir, "The role of vegetable oil in water based phase change materials for medium temperature refrigeration," *J. Energy Storage*, vol. 15, pp. 368–378, 2018, doi: 10.1016/j.est.2017.12.014.
- [5] H. Zhu, S. Hu, G. Wang, L. Han, M. Jing, and X. Zhao, "Full-scale numerical simulation and experimental validation of the thermal environment under the heating mode in an air-conditioned room," *Case Stud. Therm. Eng.*, vol. 51, no. July, p. 103548, 2023, doi: 10.1016/j.csite.2023.103548.
- [6] M. Hamed Alhamdo, M. Abdulwahed Theeb, and J. Jaber Abdulhameed, "Performance Improvement of an Air-Conditioning System During Refrigerant Evaporation," *J. Eng. Sustain. Dev.*, vol. 2018, no. 06, pp. 101–113, 2018, doi: 10.31272/jeasd.2018.6.9.
- [7] Á. Andrade, Á. Restrepo, and J. E. Tibaquirá, "EER or Fcsp: A performance analysis of fixed and variable air conditioning at different cooling thermal conditions," *Energy Reports*, vol. 7, pp. 537–545, 2021, doi: 10.1016/j.egy.2020.12.041.

- [8] S. Sheng, T. Yamanaka, T. Kobayashi, N. Choi, and S. Yodono, "Draft-free air conditioning through split membrane ceiling system\_ An exploratory study," *Indoor Environ.*, vol. 1, no. 2, p. 100017, 2024, doi: 10.1016/j.indenv.2024.100017.
- [9] D. Lee and S. T. Lee, "Artificial intelligence enabled energy-efficient heating, ventilation and air conditioning system: Design, analysis and necessary hardware upgrades," *Appl. Therm. Eng.*, vol. 235, no. July, p. 121253, 2023, doi: 10.1016/j.applthermaleng.2023.121253.
- [10] S. Alshammari, S. T. Kadam, and Z. Yu, "Assessment of single rotor expander-compressor device in combined organic Rankine cycle ( ORC ) and vapor compression refrigeration cycle ( VCR )," vol. 282, no. January, 2023.
- [11] S. A. Bhat *et al.*, "Experiments and modeling on thermal performance evaluation of standalone and M-cycle based desiccant air-conditioning systems," *Energy Reports*, vol. 11, no. October 2023, pp. 1445–1454, 2024, doi: 10.1016/j.egy.2024.01.019.
- [12] C. Liang, F. Zha, and X. Li, "Low-grade energy-bus air conditioning system using energy efficient three-fluid heat exchange terminals," *Next Energy*, vol. 3, no. October 2023, p. 100098, 2024, doi: 10.1016/j.nxener.2024.100098.
- [13] M. H. Alhamdo, M. A. Theeb, and J. J. Abdulhameed, "Using Evaporative Cooling Methods for Improving Performance of an Air-cooled Condenser," *Univers. J. Mech. Eng.*, vol. 3, no. 3, pp. 94–106, 2015, doi: 10.13189/ujme.2015.030304.
- [14] M. Schweizer, M. Stöckl, R. Tutunaru, and U. Holzhammer, "Influence of heating, air conditioning and vehicle automation on the energy and power demand of electromobility," *Energy Convers. Manag. X*, vol. 20, no. June, 2023, doi: 10.1016/j.ecmx.2023.100443.
- [15] T. Yamamoto, A. Ozaki, K. Aratsu, and R. Fukui, "Energy simulation and CFD coupled analysis for the optimal operation of combined convection and radiant air conditioning considering dehumidification," *Heliyon*, vol. 9, no. 7, p. e18092, 2023, doi: 10.1016/j.heliyon.2023.e18092.
- [16] H. Omar *et al.*, "Influence of the process and regeneration air conditions on the thermal performance of various desiccant air-conditioning systems," *Energy Convers. Manag. X*, vol. 22, no. March, p. 100582, 2024, doi: 10.1016/j.ecmx.2024.100582.
- [17] D. Saad and M. S. Kassim, "Effect of Baffles Geometry on Heat Transfer Enhancement inside Corrugated Duct," *Int. J. Mech. Eng. Technol.*, vol. 10, no. 03, pp. 555–566, 2019, [Online]. Available: <http://www.iaeme.com/IJMET/index.asp555http://www.iaeme.com/ijmet/issues.asp?JType=IJMET&VType=10&IType=3h>  
<http://www.iaeme.com/IJMET/issues.asp?JType=IJMET&VType=10&IType=3>
- [18] H. Zhang, C. Fan, T. Xiong, G. Liu, and G. Yan, "Improving performance of air conditioning system by using variable-circuit heat exchanger: Based on the Chinese APF standard," *Case Stud. Therm. Eng.*, vol. 50, no. August, p. 103422, 2023, doi: 10.1016/j.csite.2023.103422.
- [19] J. Li and B. Li, "Scenario analysis of hydrofluorocarbons consumption and emission reduction in China's mobile air-conditioning sector," *Energy Reports*, vol. 11, no. February, pp. 3171–3185, 2024, doi: 10.1016/j.egy.2024.02.026.
- [20] A. Andrade, J. Zapata-Mina, and A. Restrepo, "Exergy and environmental assessment of R-290 as a substitute of R-410A of room air conditioner variable type based on LCCP and TEWI approaches," *Results Eng.*, vol. 21, no. November 2023, p. 101806, 2024, doi: 10.1016/j.rineng.2024.101806.
- [21] A. Esmaeel, A. Rahimnejad, and S. A. Gadsden, "Home energy management system for smart buildings with inverter-based air conditioning system," *Int. J. Electr. Power Energy Syst.*, vol. 133, no. August 2020, p. 107230, 2021, doi: 10.1016/j.ijepes.2021.107230.
- [22] L. Zhu, J. Hong, S. Yang, Z. Hu, Y. Shao, and C. Wu, "Online modeling of virtual energy storage for inverter air conditioning clusters in CDL-based demand response," *Energy Reports*, vol. 9, no. 2023, pp. 2024–2034, 2024, doi: 10.1016/j.egy.2023.04.169.
- [23] S. Liu, W. Ge, and X. Meng, "Influence of the shading nets on indoor thermal environment and air-conditioning energy consumption in lightweight buildings," *Energy Reports*, vol. 11, no. April, pp. 4515–4521, 2024, doi: 10.1016/j.egy.2024.04.032.
- [24] Y. Ding and J. Fournier, "Modeling and analysis of inverter air conditioners for primary 15th analysis Modeling and air conditioners for primary frequency control considering signal delays and detection errors frequency control considering signal delays and detection errors Assess," *Energy Procedia*, vol. 158, pp. 4003–4010, 2019, doi: 10.1016/j.egypro.2019.01.840.
- [25] R. Conte, M. Azzolin, S. Bernardinello, and D. Del Col, "Experimental investigation of large scroll compressors working with six low-GWP refrigerants," *Therm. Sci. Eng. Prog.*, vol. 44, no. July, p. 102043, 2023, doi: 10.1016/j.tsep.2023.102043.
- [26] J. Bai *et al.*, "Experimental study of phase change heat dissipation system based on hydrogen fuel cell," *Case Stud. Therm. Eng.*, vol. 59, no. May, p. 104495, 2024, doi: 10.1016/j.csite.2024.104495.
- [27] F. Guo, Z. Chen, and F. Xiao, "Fault detection and diagnosis of electric bus air conditioning systems incorporating domain knowledge and probabilistic artificial intelligence," *Energy AI*, vol. 16, no. March, p. 100364, 2024, doi: 10.1016/j.egyai.2024.100364.
- [28] W. Watcharajinda, A. Asanakham, T. Deethayat, and T. Kiatsiriroat, "Performance study of open pond as heat sink of water-cooled air conditioner," *Case Stud. Therm. Eng.*, vol. 25, no. January, p. 100988, 2021, doi: 10.1016/j.csite.2021.100988.
- [29] A. S. Kvalsund and D. Winkler, "Development of an Arduino-based , open-control interface for hardware in the loop applications," *HardwareX*, vol. 16, no. October, p. e00488, 2023, doi: 10.1016/j.ohx.2023.e00488.
- [30] B. Nast, A. Reiz, and K. Sandkuhl, "Iot-based diagnostic assistance for energy optimization of air conditioning facilities," *Procedia Comput. Sci.*, vol. 219, no. 2022, pp. 416–421, 2023, doi: 10.1016/j.procs.2023.01.307.
- [31] A. Abolore, D. Olurotimi, O. Edward, H. Olajumoke, and F. Nihinlola, "Arduino microcontroller based real-time monitoring of haemodialysis process for patients with kidney disease," *e-Prime - Adv. Electr. Eng. Electron. Energy*, vol. 7, no. November 2023, p. 100403, 2024, doi: 10.1016/j.pprime.2023.100403.
- [32] K. Confidence, L. Bokopane, and K. Kusakana, "Real-time power dispatch in a standalone hybrid multisource distributed energy system using an Arduino board," *Energy Reports*, vol. 7, pp. 479–486, 2021, doi: 10.1016/j.egy.2021.08.016.
- [33] J. Ham, Y. Shin, M. Lee, and H. Cho, "Investigation of performance and energy cost of automobile air-conditioner using alternative refrigerants based on thermal comfort using various cooling seats," *Results Eng.*, vol. 20, no. October, p. 101541, 2023, doi: 10.1016/j.rineng.2023.101541.
- [34] P. Sphicas and A. Pesyridis, "Investigation of the temporal behavior of desiccant disk for use in dehumidifiers and air conditioners," *Results Eng.*, vol. 21, no. December 2023, p. 101801, 2024, doi: 10.1016/j.rineng.2024.101801.
- [35] J. J. Abdulhameed, M. S. Kassim, and M. S. Kadhim, "Experimental investigation of a condenser air humidity effect on superheated degree of compressor," *J. Mech. Eng. Res. Dev.*, vol. 44, no. 5, pp. 167–176, 2021.

- [36] A. Y. Sulaiman *et al.*, “A solar powered off-grid air conditioning system with natural refrigerant for residential buildings: A theoretical and experimental evaluation,” *Clean. Energy Syst.*, vol. 5, no. June, 2023, doi: 10.1016/j.cles.2023.100077.
- [37] G. K. Murugesan, C. Murugesan, and S. Tamilkolundu, “Assessment of performance and sustainability of waste heat dryer coupled with air conditioner unit during drying of banana slices,” *Case Stud. Therm. Eng.*, vol. 59, no. May, p. 104506, 2024, doi: 10.1016/j.csite.2024.104506.
- [38] M. Marwan *et al.*, “Temperature Control Strategy to Mitigate Electrical Energy Cost for Air Conditioning,” *e-Prime - Adv. Electr. Eng. Electron. Energy*, vol. 7, no. October 2023, p. 100410, 2024, doi: 10.1016/j.prime.2023.100410.
- [39] C. Chen, H. Yang, X. Li, L. Chen, and M. Shi, “Optimization of solar and heat pump complementary powered desiccant air conditioning system,” *J. Build. Eng.*, vol. 87, no. March, p. 109084, 2024, doi: 10.1016/j.jobee.2024.109084.
- [40] P. Zi *et al.*, “Modeling method of variable frequency air conditioning load,” *Energy Reports*, vol. 9, pp. 1011–1017, 2023, doi: 10.1016/j.egy.2022.11.035.
- [41] F. Guo, Z. Chen, and F. Xiao, “Fault detection and diagnosis of electric bus air conditioning systems incorporating domain knowledge and probabilistic artificial intelligence,” *Energy AI*, vol. 16, no. March, p. 100364, 2024, doi: 10.1016/j.egy.2024.100364.
- [42] A. Venkateshvaran *et al.*, “A novel echocardiographic estimate of pulmonary vascular resistance employing the hydraulic analogy to Ohm ’ s law ☆,” *IJC Hear. Vasc.*, vol. 42, no. September, p. 101121, 2022, doi: 10.1016/j.ijcha.2022.101121.
- [43] P. L. C. Chua *et al.*, “Net impact of air conditioning on heat-related mortality in Japanese cities,” *Environ. Int.*, vol. 181, no. October, p. 108310, 2023, doi: 10.1016/j.envint.2023.108310.
- [44] K. Z. ZHAO and Z. Y. SU, “Experimental study on refrigeration system performance of pure electric refrigerator car based on medium pressure air supply,” *e-Prime - Adv. Electr. Eng. Electron. Energy*, vol. 7, no. October 2023, p. 100399, 2024, doi: 10.1016/j.prime.2023.100399.